SIAM J. NUMER. ANAL.
Vol. 35, No. 5, pp. 1850–1861, October 1998

008

MIXED COVOLUME METHODS FOR ELLIPTIC PROBLEMS ON TRIANGULAR GRIDS*

SO-HSIANG CHOU†, DO Y. KWAK‡, AND PANAYOT S. VASSILEVSKI§

Abstract. We consider a covolume or finite volume method for a system of first-order PDEs resulting from the mixed formulation of the variable coefficient-matrix Poisson equation with the Neumann boundary condition. The system may represent either the Darcy law and the mass conservation law in anisotropic porous media flow, or Fourier law and energy conservation. The velocity and pressure are approximated by the lowest order Raviart–Thomas space on triangles. We prove its first-order optimal rate of convergence for the approximate velocities in the L^2-and $H(\text{div};\Omega)$-norms as well as for the approximate pressures in the L^2-norm. Numerical experiments are included.

Key words. MAC method, mixed finite elements, covolume methods, finite volume methods, Raviart–Thomas spaces, error estimates, preconditioning, hierarchical methods

AMS subject classifications. 65F10, 65N20, 65N30

PII. S0036142997321285

1. Introduction. Consider the variable coefficient Poisson equation in a polygonal domain $\Omega \subset R^2$

$$\left\{ \begin{array}{rcl} -\nabla \cdot \mathcal{K}\nabla p &=& f \text{ in } \Omega, \\ \mathcal{K}\nabla p \cdot \mathbf{n} &=& 0 \text{ in } \partial\Omega, \end{array} \right. \tag{1.1}$$

where $\mathcal{K} = \mathcal{K}(\mathbf{x}) = \text{diag}(\tau_1^{-1}(\mathbf{x}), \tau_2^{-1}(\mathbf{x}))$ is a symmetric positive definite diagonal matrix function and its entries are bounded from below and above by positive constants. The function f satisfies the compatibility condition $\int_\Omega f dx = 0$. Furthermore, we shall assume that τ_1, τ_2 are locally Lipschitz.

Let us introduce a new variable $\mathbf{u} = -\mathcal{K}\nabla p$ and write the above equation as the system of first-order partial differential equations

$$\left\{ \begin{array}{rcl} \mathcal{K}^{-1}\mathbf{u} &=& -\nabla p, \\ \text{div}\mathbf{u} &=& f, \\ \mathbf{u} \cdot \mathbf{n} &=& 0 \text{ on } \partial\Omega. \end{array} \right. \tag{1.2}$$

This system can be interpreted as modeling an incompressible single phase flow in a reservoir, ignoring gravitational effects. The matrix $\mathcal{K}$ is the mobility κ/μ, the ratio of permeability tensor to viscosity of the fluid—$\mathbf{u}$ is the Darcy velocity and p the pressure. The first equation is the Darcy law and the second represents conservation of mass with f standing for a source or sink term. Since κ is in general discontinuous

*Received by the editors May 9, 1997; accepted for publication (in revised form) January 6, 1998; published electronically August 13, 1998.
http://www.siam.org/journals/sinum/35-5/32128.html

†Department of Mathematics and Statistics, Bowling Green State University, Bowling Green, OH 43403-0221 (chou@zeus.bgsu.edu).

‡Department of Mathematics, Korea Advanced Institute of Science and Technology, Taejon, Korea 305-701 (dykwak@math.kaist.ac.kr). The work of this author was supported by KOSEF, Korea. Part of the research of this author was done while visiting the Department of Mathematics and Statistics at Bowling Green State University.

§Center of Informatics and Computing Technology, Bulgarian Academy of Sciences, "Acad. G. Bontchev" Street, Block 25 A, 1113 Sofia, Bulgaria (panayot@iscbg.acad.bg). The work of this author was supported by the Bulgarian Ministry for Education, Science and Technology under grant I-95 # 504. Part of the research of this author was done while visiting the Department of Mathematics and Statistics at Bowling Green State University.

due to different rock formations, separating the Darcy law from the second-order equation and discretizing it directly together with the mass conservation may lead to a better numerical treatment on the velocity than just computing it from the pressure via the Darcy law. This approach is well known in the finite element circle [19], but the same approach can be applied in conjunction with the finite volume method as well (see [4, 7, 10, 20]).

The associated weak formulation of our first-order system is: Find $(\mathbf{u}, p) \in \mathbf{H}_0 \times L_0^2$ such that

$$
\begin{array}{rcll}
(\mathcal{K}^{-1}\mathbf{u}, \mathbf{v}) & = & (p, \operatorname{div} \mathbf{v}), & \forall \mathbf{v} \text{ in } \mathbf{H}_0, \\
(\operatorname{div}\mathbf{u}, q) & = & (f, q), & \forall q \text{ in } L_0^2,
\end{array}
\tag{1.3}
$$

where $\mathbf{H}_0 := H(\operatorname{div}; \Omega) \cap \{\mathbf{u} \cdot \mathbf{n} = 0\}$ and $L_0^2 := \{q \in L^2 : \int_\Omega q dx = 0\}$. The space $H(\operatorname{div}; \Omega)$ is the set of all vector-valued functions $\mathbf{w} \in L^2(\Omega)^2$ such that $\operatorname{div} \mathbf{w} \in L^2(\Omega)$.

We will use a covolume method to approximate this system. In a covolume method for differential systems one uses two staggered irregular grids—a primal grid consisting of primal volumes (elements) and a dual grid consisting of covolumes (dual elements). The associated discretization equations are derived by integrating the differential equations over the volumes and using the divergence theorem or the Stokes theorem when proper. The balance between the numbers of unknowns and equations depends on a judicious placement of the degrees of freedom for the unknown functions. A well-known example of this approach in the fluid dynamics is the marker and cell (MAC) method [14] on staggered rectangular grids for the Navier–Stokes equations. In the MAC method one places the velocity degree of freedom on the boundary of the volumes in the primal partition and the pressure degree of freedom at the centers. The MAC method actually preceded the covolume method, and there are many generalizations of the MAC method to irregular grids, e.g., [13, 15, 16] for the Navier–Stokes equations, among others. In our covolume method we will adopt the same type of MAC variable placement for the pressure and velocity variables, although we are not dealing with the Navier–Stokes equations. The covolume approach can also be applied to other systems such as the div-curl system arising from the Maxwell equations. We refer the reader to the survey paper by Nicolaides, Porsching, and Hall [17] for other applications and status of the covolume method up to 1995. The reader can also find therein other interpretations of the covolume approach.

One recent emphasis in the development has been to put the convergence and stability analysis of the covolume method into a general framework [5, 6, 7, 8, 9, 10]. In these papers the covolume method was viewed as a Petrov–Galerkin scheme. The basic technique was to relate the scheme to a standard finite element Galerkin or mixed method through an introduction of the transfer operator that maps the trial function space into the test function space. However, the transfer operator played no essential role in the implementation of the method itself.

The purpose of this paper is to consider a covolume method on triangular-quadrilateral grids which makes essential use of the transfer operator. In other words, the operator is not only used as an analysis tool, but also defines the scheme itself. To ease the description let us define two partitions on the domain Ω, a primal partition over which to integrate the continuity equation, and a dual partition for integrating the Darcy law.

Referring to Fig. 1, let $T_h = \{K_B\}$ be a partition of the domain Ω into a union of triangular elements, where K_B stands for the triangle whose barycenter is B. We define the nodes of a triangular element to be its midpoints and denote by $P_1, P_2, \ldots, P_{N_S}$ those nodes belonging to the interior of Ω and $P_{N_S+1}, \ldots, P_N$ those

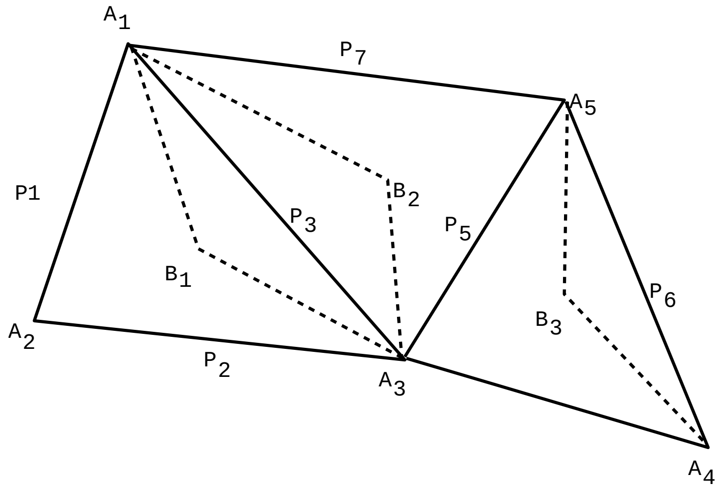

FIG. 1. *Primal and dual domains.*

nodes on the boundary. The *trial* function space $\mathbf{H}_h$ associated with the approximation of the fluid velocity is the lowest-order Raviart–Thomas space for triangles, i.e.,

$$\mathbf{H}_h := \{\mathbf{v}_h \in \mathbf{H}_0 : \mathbf{v}_h|_K = (a + bx, c + by),\ K \in T_h\},$$

and the trial space associated with the pressure is

$$L_h := \{q_h \in L^2_0 : q_h|_K \text{ is constant } \forall K \in T_h\}.$$

Next we construct the dual partition T_h^* and the test function space. The dual grid is a union of interior quadrilaterals and border triangles. Referring to Fig. 1, the interior node P_3 belongs to the common side of the triangles $K_{B_1} = \Delta A_1A_2A_3$ and $K_{B_2} = \Delta A_1A_3A_5$, and the quadrilateral $A_1B_2A_3B_1$ is the dual element with node at P_3. For a boundary node like P_6 the associated dual element is a triangle ($\Delta A_5B_3A_4$ in this case).

In general, let K_p^* (dashed quadrilateral in Fig. 1) be an interior dual element that is the union of two primal elements K_L (the triangle $\Delta A_1B_2A_3$ in Fig. 1) and K_R (the triangle $\Delta A_1B_2A_3$). Define the operator $\gamma_h : \mathbf{H}_h \to L^2(\Omega)^2$

$$\gamma_h \mathbf{w_h} = \sum_{j=1}^{N_S} \left(\mathbf{w}_h|_{K_L}(P_j)\chi_{K_j^* \cap K_L} + \mathbf{w}_h|_{K_R}(P_j)\chi_{K_j^* \cap K_R} \right), \tag{1.4}$$

where χ_Q is the characteristic function of the set Q and N_S is the number of interior edges of T_h. The test space associated with the Darcy law is defined as

$$\mathbf{Y}_h := R(\gamma_h) = \text{the range of } \gamma_h.$$

Thus, by (1.4) a function $\mathbf{w}_h \in \mathbf{Y}_h$ is a piecewise constant vector function, which can take on different constant vector values on the left and right pieces of an interior dual element and is zero on any boundary dual element. Note that the two constant vector values $\mathbf{w}_h|_{K_L}$ and $\mathbf{w}_h|_{K_R}$ must satisfy

$$\mathbf{w}_h|_{K_L} \cdot \mathbf{n} = \mathbf{w}_h|_{K_R} \cdot \mathbf{n},$$

where $\mathbf{n}$ is a fixed normal unit vector to the common edge of K_L and K_R. It is now easy to see that the *transfer* operator γ_h sets up a one-to-one correspondence between the trial and test spaces and $\dim \mathbf{Y}_h = \dim \mathbf{H}_h$. We mention in passing that the space $\mathbf{Y}_h$ is also very natural for defining upwinding mixed finite volume methods [10, 11, 12].

The standard mixed method on the primal grid is: Find $(\tilde{\mathbf{u}}_h, \tilde{p}_h) \in \mathbf{H}_h \times L_h$ such that

$$\begin{aligned} (\mathcal{K}^{-1}\tilde{\mathbf{u}}_h, \mathbf{v}_h) - (\mathrm{div}\mathbf{v}_h, \tilde{p}_h) &= 0, \quad \forall \mathbf{v}_h \text{ in } \mathbf{H}_h, \\ (\mathrm{div}\tilde{\mathbf{u}}_h, q_h) &= (f, q_h), \quad \forall q_h \text{ in } L_h. \end{aligned} \tag{1.5}$$

A natural Petrov–Galerkin method which corresponds to the above method and which obeys the MAC placement of variables is to replace $\mathbf{v}_h \in \mathbf{H}_h$ by $\mathbf{w}_h \in \mathbf{Y}_h$. To this end, let us define the bilinear forms $a(\cdot,\cdot)$ on $\mathbf{H}_h \times \mathbf{Y}_h$, $b(\cdot,\cdot)$ on $\mathbf{Y}_h \times L_h$, and $c(\cdot,\cdot)$ on $\mathbf{H}_h \times L_h$ as follows:

$$a(\mathbf{v}_h, \mathbf{w}_h) := \int_\Omega \mathcal{K}^{-1}\mathbf{v}_h \cdot \mathbf{w}_h d\mathbf{x}, \quad \mathbf{v}_h \in \mathbf{H}_h, \mathbf{w}_h \in \mathbf{Y}_h, \tag{1.6}$$

$$\begin{aligned} b(\mathbf{w}_h, p_h) = & -\sum_1^{N_S} \mathbf{v}_h(P_i)|_{K_L} \cdot \int_{\partial K^*_{P_i} \cap K_L} q_h \mathbf{n} d\sigma \\ & -\sum_1^{N_S} \mathbf{v}_h(P_i)|_{K_R} \cdot \int_{\partial K^*_{P_i} \cap K_R} q_h \mathbf{n} d\sigma, \end{aligned} \tag{1.7}$$

$$c(\mathbf{v}_h, q_h) = \sum_{k=1}^{T} q_h(B_k) \int_{K_B} \mathrm{div}\mathbf{v}_h d\mathbf{x} \tag{1.8}$$

$$= \int_\Omega q_h \mathrm{div} q_h d\mathbf{x}. \tag{1.9}$$

Then the covolume method we consider is: Find $(\mathbf{u}_h, p_h) \in \mathbf{H}_h \times L_h$ such that

$$\begin{aligned} a(\mathbf{u}_h, \gamma_h \mathbf{v}_h) + b(\gamma_h \mathbf{v}_h, p_h) &= 0, \qquad \forall \mathbf{v}_h \text{ in } \mathbf{H}_h, \\ c(\mathbf{u}_h, q_h) &= (f, q_h), \quad \forall q_h \text{ in } L_h. \end{aligned} \tag{1.10}$$

Set

$$A(\mathbf{u}_h, \mathbf{v}_h) := a(\mathbf{u}_h, \gamma_h \mathbf{v}_h) = (\mathcal{K}^{-1}\mathbf{u}_h, \gamma_h \mathbf{v}_h), \quad \mathbf{u}_h, \mathbf{v}_h \in \mathbf{H}_h \tag{1.11}$$

and

$$B(\mathbf{v}_h, q_h) = b(\gamma_h \mathbf{v}_h, q_h), \quad \forall \mathbf{v}_h \in \mathbf{H}_h, q_h \in L_h. \tag{1.12}$$

We show in Lemma 2.1 that $B = -c$ so that (1.10) becomes

$$A(\mathbf{u}_h, \mathbf{w}_h) + B(\mathbf{w}_h, p_h) = 0, \quad \forall \mathbf{w}_h \text{ in } \mathbf{H}_h, \tag{1.13}$$

$$B(\mathbf{u}_h, q_h) = -(f, q_h), \quad \forall q_h \text{ in } L_h, \tag{1.14}$$

which differs from the standard mixed method (1.5) only in the bilinear form A. The first-order convergence of the solutions of (1.13)–(1.14) is established in Theorem 3.1 by comparing the two methods.

The organization of this paper is as follows. In section 2 we establish some preliminary lemmas. We prove our main theorem in section 3, which demonstrates the first-order convergence of the velocity in the $H(\mathrm{div})$ norm and of the pressure in the L^2-norm. We provide numerical results in the last section and compare them with the standard mixed method.

2. Saddle-point formulation. In this section the symbol C will denote a positive generic constant independent of h that may take on different values in different places.

LEMMA 2.1. *The following holds.*

$$B(\mathbf{v}_h, q_h) = b(\gamma_h \mathbf{v}_h, q_h) = -c(\mathbf{v}_h, q_h), \qquad \forall \mathbf{v}_h \in \mathbf{H}_h, q_h \in L_h.$$

Proof.

$$\begin{aligned} -B(\mathbf{v}_h, q_h) &= \sum_1^{N_S} \left(\mathbf{v}_h(P_i)|_{K_L} \cdot \int_{\partial K^*_{P_i} \cap K_L} q_h \mathbf{n} d\sigma + \mathbf{v}_h(P_i)|_{K_R} \cdot \int_{\partial K^*_{P_i} \cap K_R} q_h \mathbf{n} d\sigma \right) \\ &= \sum_{K \in T_h} I_K. \end{aligned}$$

Then

$$\begin{aligned} I_K &= \sum_{j=1}^{3} \int_{A_{j+1}BA_j} q_h \mathbf{v}_h(P_j) \cdot \mathbf{n} d\sigma \\ &= \sum_{j=1}^{3} \left[\int_{\Delta A_{j+1}BA_j} \mathrm{div}\,(q_h \mathbf{v}_h(P_j)) d\sigma - \int_{A_j A_{j+1}} q_h \mathbf{v}_h(P_j) \cdot \mathbf{n} d\sigma \right] \\ &= \sum_{j=1}^{3} \left[0 - \int_{A_j A_{j+1}} q_h \mathbf{v}_h(P_j) \cdot \mathbf{n} d\sigma \right] \\ &= -\sum_{j=1}^{3} (q_h \mathbf{v}_h(P_j) \cdot \mathbf{n}) |A_j A_{j+1}| \\ &= -\sum_{j=1}^{3} q_h \left(\frac{\mathbf{v}_h(A_j) + \mathbf{v}_h(A_{j+1})}{2} \right) \cdot \mathbf{n} |A_j A_{j+1}| \\ &= -\sum_{j=1}^{3} \int_{A_j A_{j+1}} q_h \mathbf{v}_h(\mathbf{x}) \cdot \mathbf{n} d\sigma \\ &= -q_h \int_K \mathrm{div}\,(\mathbf{v}_h(\mathbf{x}))\, d\mathbf{x}. \qquad \square \end{aligned}$$

We next show the coercivity of A.

LEMMA 2.2. *There exists a constant C independent of h such that*

$$A(\mathbf{v}_h, \mathbf{v}_h) \geq C \|\mathbf{v}_h\|^2_{H(\mathrm{div})}, \qquad \forall \mathbf{v} \in \mathbf{H}_h$$

with $\mathrm{div}\mathbf{v}_h = 0$.

Proof. Since on each K, $\mathbf{v}_h$ is of the form $(a + bx, c + by)$, $\mathrm{div}\mathbf{v}_h = 0$ implies $b = 0$. Thus we have $\mathbf{u}_h = (a, c)$ and $\gamma \mathbf{u}_h = \mathbf{u}_h$ on K and the result is trivial. $\square$

Then the problem becomes

$$A(\mathbf{u}_h,\mathbf{w}_h)+B(\mathbf{w}_h,p_h) \;=\; 0, \quad \forall \mathbf{w}_h \text{ in } \mathbf{H}_h, \tag{2.1}$$

$$B(\mathbf{u}_h,q_h) \;=\; -(f,q_h), \quad \forall q_h \text{ in } L_h(\Omega). \tag{2.2}$$

Now by Lemma 2.1, B becomes a well-known bilinear form and we have the following inf-sup condition.

LEMMA 2.3. *There exists a positive constant β independent of h such that*

$$\sup_{\mathbf{w}_h\neq 0}\frac{B(\mathbf{w}_h,q_h)}{|\mathbf{w}_h|_{H(\mathrm{div})}}\geq \beta\|q_h\|_0. \tag{2.3}$$

Note that by the previous lemmas and the boundedness of A and B, the covolume method (2.1)–(2.2) is well posed. Next we show some crucial approximation properties of γ_h. Let us first define a discrete seminorm for $\mathbf{w}_h=(w_h,v_h)\in\mathbf{H}_h$:

$$|\mathbf{w}_h|_{1,h}^2 := \sum_{K\in T_h}||\nabla w_h||_{0,K}^2+||\nabla v_h||_{0,K}^2 \tag{2.4}$$

and the full norm

$$||\mathbf{w}_h||_{1,h}^2=||\mathbf{w}_h||_0^2+|\mathbf{w}_h|_{1,h}^2.$$

We also use $||\mathbf{w}_h||_{1,h;K}$ for the corresponding restriction. Since the bilinear form $a(\cdot,\cdot)$ of (1.6) involves only L^2-functions, we can extend it accordingly.

LEMMA 2.4. *The transfer operator γ_h is bounded*

$$\|\gamma_h\mathbf{w}_h\|_0\leq\|\mathbf{w}_h\|_0, \quad \forall\mathbf{w}_h\in\mathbf{H}_h. \tag{2.5}$$

There exists a constant C independent of h such that

$$\|(I-\gamma_h)\mathbf{w}_h\|_0\leq Ch||\mathbf{w}_h||_{1,h}, \quad \forall\mathbf{w}_h\in\mathbf{H}_h, \tag{2.6}$$

$$|(\gamma_h\mathbf{u}_h,\mathbf{w}_h)-(\mathbf{u}_h,\gamma_h\mathbf{w}_h)|\leq Ch\left(|\mathbf{u}_h|_{H(\mathrm{div})}\|\mathbf{w}_h\|_0+\|\mathbf{u}_h\|_0|\mathbf{w}_h|_{H(\mathrm{div})}\right), \tag{2.7}$$

$$a(\mathbf{u}_h,(I-\gamma_h)\mathbf{w}_h)\leq Ch||\mathbf{u}_h||_{1,h}||\mathbf{w}_h||_{H(\mathrm{div})}, \qquad \forall\mathbf{u}_h,\mathbf{w}_h\in\mathbf{H}_h, \tag{2.8}$$

$$a(\mathbf{u}_h,(I-\gamma_h)\mathbf{w}_h)\leq Ch||\mathbf{u}_h||_{H(\mathrm{div})}||\mathbf{w}_h||_{H(\mathrm{div})}, \qquad \forall\mathbf{u}_h,\mathbf{w}_h\in\mathbf{H}_h. \tag{2.9}$$

Proof. The relation (2.5) is easily proved by noting that the midpoint quadrature rule

$$\int_K\phi dx=\frac{1}{3}|K|\sum_{i=1}^{3}\phi(P_i),$$

where P_i are the midpoints of sides of K, is exact for quadratic polynomials. Now with $K=A_1A_2A_3$ denoting a typical triangle (cf. Fig. 2), $\Delta_j=\Delta A_{j+1}BA_j$, we have

$$\|\gamma\mathbf{w}_h\|_0^2=\int\left|\sum_{j=1}^{N_S}\mathbf{w}_h\Big|_{K_L}(P_j)\chi^*_{K_j^*\cap K_L}+\mathbf{w}_h\Big|_{K_R}(P_j)\chi^*_{K_j^*\cap K_R}\right|^2dx \tag{2.10}$$

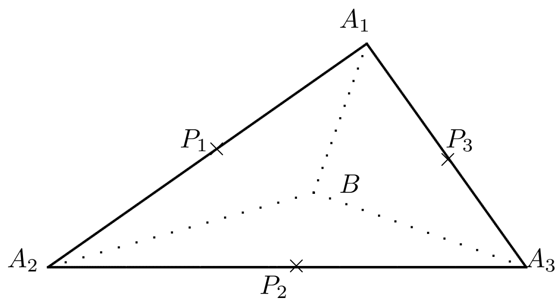

FIG. 2. *An element K and its dual subdivision.*

$$
\begin{aligned}
&\le \sum_K \sum_{j=1}^{3} |\mathbf{w}_{h,K}(P_j)|^2 Area(\Delta_j) \\
&= \sum_K \frac{1}{3} \sum_{j=1}^{3} |\mathbf{w}_{h,K}(P_j)|^2 Area(K) \\
&\le \|\mathbf{w}_h\|_0^2.
\end{aligned}
$$

The proof of (2.6) is straightforward by the Bramble–Hilbert lemma.

To prove (2.7), let $K = A_1A_2A_3$, (cf. Fig. 2), $\Delta_j = \Delta A_{j+1}BA_j$, and c_j be the centroid of Δ_j. Then

$$
\begin{aligned}
(\mathbf{u}_h, \gamma_h\mathbf{w}_h)_{\Delta_j} &- (\gamma_h\mathbf{u}_h, \mathbf{w}_h)_{\Delta_j} \\
&= \int_{\Delta_j} [\mathbf{u}_h(x)\mathbf{w}_h(P_j) - \mathbf{u}_h(P_j)\mathbf{w}_h(x)]dx \\
&= [\mathbf{u}_h(c_j)\mathbf{w}_h(P_j) - \mathbf{u}_h(P_j)\mathbf{w}_h(c_j)]Area(\Delta_j) \\
&= [(\mathbf{u}_h(c_j) - \mathbf{u}_h(P_j)) \cdot \mathbf{w}_h(P_j) + \mathbf{u}_h(P_j) \cdot (\mathbf{w}_h(P_j) - \mathbf{w}_h(c_j))]Area(\Delta_j) \\
&= [D\mathbf{u}_h(c_j - P_j) \cdot \mathbf{w}_h(P_j) + \mathbf{u}_h(P_j) \cdot D\mathbf{w}_h(P_j - c_j)]Area(\Delta_j) \\
&= \frac{1}{2} (\mathrm{div}\mathbf{u}_h(c_j - P_j) \cdot \mathbf{w}_h(P_j) + \mathrm{div}\mathbf{w}_h(P_j - c_j) \cdot \mathbf{u}_h(P_j))\, Area(\Delta_j) \\
&\le Ch\,(|\mathrm{div}\mathbf{u}_h||\mathbf{w}_h(P_j)| + |\mathrm{div}\mathbf{w}_h||\mathbf{u}_h(P_j)|)\, Area(\Delta_j) \\
&\le Ch\left(|\mathbf{u}_h|_{H(\mathrm{div}),\Delta_j}\|\mathbf{w}_h\|_K + \|\mathbf{u}_h\|_K|\mathbf{w}_h|_{H(\mathrm{div}),\Delta_j}\right).
\end{aligned}
$$

Summing over all j and K, we obtain (2.7).

To prove (2.8), observe

$$
\begin{aligned}
a(\mathbf{u}_h, (I - \gamma_h)\mathbf{w}_h) &= a((I - \gamma_h)\mathbf{u}_h, \mathbf{w}_h) + [a(\gamma_h\mathbf{u}_h, \mathbf{w}_h) - a(\mathbf{u}_h, \gamma_h\mathbf{w}_h)] \\
&= S_1 + S_2.
\end{aligned}
$$

We shall show that S_1 and S_2 are bounded by the right-hand side of (2.8). For S_1, first note that by (2.6)

$$
\begin{aligned}
|S_1| &= |a((I - \gamma_h)\mathbf{u}_h, \mathbf{w}_h)| \\
&= |(\mathcal{K}^{-1}(I - \gamma_h)\mathbf{u}_h, \mathbf{w}_h)| \\
&= |((I - \gamma_h)\mathbf{u}_h, \mathcal{K}^{-1}\mathbf{w}_h)| \\
&\le C||\mathcal{K}^{-1}||_\infty h||\mathbf{u}_h||_{1,h}\|\mathbf{w}_h\|.
\end{aligned}
$$

We next show how to bound S_2. Write $\mathcal{K}^{-1}$ =diag$(\tau_1(\mathbf{x}), \tau_2(\mathbf{x}))$ with $0 < t_{\min} \leq \tau_1, \tau_2 \leq t_{\max}$. We need to estimate

$$\sum_K \sum_{j=1}^{3} (\mathcal{K}^{-1}\gamma_h \mathbf{u}_h, \mathbf{w}_h)_{\Delta_j} - (\mathcal{K}^{-1}\mathbf{u}_h, \gamma_h \mathbf{w}_h)_{\Delta_j}.$$

Now by (2.6), Lipschitz continuity of $\mathcal{K}^{-1}$, and (2.7), we have

$$\begin{aligned} S_2 = &\sum_K \sum_{j=1}^{3} ((\mathcal{K}^{-1}(\mathbf{x}) - \mathcal{K}^{-1}(P_j))\gamma_h \mathbf{u}_h, \mathbf{w}_h)_{\Delta_j} - ((\mathcal{K}^{-1}(\mathbf{x}) - \mathcal{K}^{-1}(P_j))\mathbf{u}_h(\mathbf{x}), \gamma_h \mathbf{w}_h(\mathbf{x}))_{\Delta_j} \\ &+ \sum_K \sum_{j=1}^{3} \mathcal{K}^{-1}(P_j) \left[(\gamma_h \mathbf{u}_h, \mathbf{w}_h)_{\Delta_j} - (\mathbf{u}_h, \gamma_h \mathbf{w}_h)_{\Delta_j} \right] \end{aligned}$$

implies

$$|S_2| \leq Mh\|\mathbf{u}_h\|_0 \|\mathbf{w}_h\|_0 + Ch\|\mathcal{K}^{-1}\|_\infty \left[|\mathbf{u}_h|_{H(\mathrm{div})} \|\mathbf{w}_h\|_0 + \|\mathbf{u}_h\| |\mathbf{w}_h|_{H(\mathrm{div})} \right],$$

where we also used the boundedness of γ_h in the L^2-norm to estimate the first term on the right. Finally, (2.9) follows from (2.8), since $||\mathbf{u}_h||_{1,h} \leq ||\mathbf{u}_h||_{H(\mathrm{div})}$, which is a direct consequence of (2.4). $\square$

3. Error estimates. We now prove the main theorem of this paper.

THEOREM 3.1. *Let the triangulation of the domain Ω be regular, and let $\{\mathbf{u}_h, p_h\}$ be the solution of the problem* (2.1)–(2.2) *and $\{\mathbf{u}, p\}$ of the problem* (1.3). *Then there exists a positive constant C independent of h but dependent on $||\mathcal{K}^{-1}||_\infty$, $\|\mathbf{u}\|_1, \|\mathrm{div}\mathbf{u}\|_1$, and $\|p\|_1$ such that*

$$\|\mathbf{u} - \mathbf{u}_h\|_{H(\mathrm{div})} + \|p - p_h\|_0 \leq Ch \tag{3.1}$$

provided that $\mathbf{u} \in \mathbf{H}^1, \mathrm{div}\,\mathbf{u} \in H^1, p \in H^1$.

Proof. Introduce the auxiliary mixed formulation to (1.3): Find $(\tilde{\mathbf{u}}_h, \tilde{p}_h) \in \mathbf{H}_h \times L_h$ such that

$$a(\tilde{\mathbf{u}}_h, \mathbf{w}_h) + B(\mathbf{w}_h, \tilde{p}_h) = 0, \quad \forall \mathbf{w}_h \text{ in } \mathbf{H}_h, \tag{3.2}$$

$$B(\tilde{\mathbf{u}}_h, q_h) = -(f, q_h), \quad \forall q_h \text{ in } L_h. \tag{3.3}$$

This system has the following well-known convergence result [18]:

$$\|\mathbf{u} - \tilde{\mathbf{u}}_h\|_{H(\mathrm{div})} + \|p - \tilde{p}_h\|_0 \leq Ch(\|\mathbf{u}\|_1 + \|\mathrm{div}\mathbf{u}\|_1 + \|p\|_1) \tag{3.4}$$

provided that $\mathbf{u} \in \mathbf{H}^1, \mathrm{div}\,\mathbf{u} \in H^1$, $p \in H^1$. On the other hand, we have

$$a(\mathbf{u}_h, \gamma_h \mathbf{w}_h) + B(\mathbf{w}_h, p_h) = 0, \quad \forall \mathbf{w}_h \in \mathbf{H}_h, \tag{3.5}$$

$$B(\mathbf{u}_h, q_h) = -(f, q_h), \quad \forall q_h \in L_h. \tag{3.6}$$

Since $\mathbf{u} - \mathbf{u}_h = (\mathbf{u} - \tilde{\mathbf{u}}_h) + (\tilde{\mathbf{u}}_h - \mathbf{u}_h)$, it suffices to estimate the second term on the right. Subtracting (3.6) from (3.3), we have

$$B(\tilde{\mathbf{u}}_h - \mathbf{u}_h, q_h) = 0, \quad \forall q_h \in L_h. \tag{3.7}$$

Subtracting (3.5) from (3.2) yields

$$a(\tilde{\mathbf{u}}_h - \mathbf{u}_h, \gamma_h \mathbf{w}_h) + a(\tilde{\mathbf{u}}_h, (I - \gamma_h)\mathbf{w}_h) + B(\mathbf{w}_h, p_h - \tilde{p}_h) = 0. \tag{3.8}$$

Replace the $\mathbf{w}_h$ above by $\tilde{\mathbf{e}}_h := \tilde{\mathbf{u}}_h - \mathbf{u}_h$ and use (3.7) to obtain

$$a(\tilde{\mathbf{e}}_h, \gamma_h \tilde{\mathbf{e}}_h) = -a(\tilde{\mathbf{u}}_h, (I - \gamma_h)\tilde{\mathbf{e}}_h).$$

By Lemma 2.2, (2.9), and (3.4)

$$\alpha \|\tilde{\mathbf{e}}_h\|^2_{H(\mathrm{div})} \le Ch \|\tilde{\mathbf{e}}_h\|_{H(\mathrm{div})},$$

where C is independent of h but dependent on $||\mathcal{K}^{-1}||_\infty$, $\|\mathbf{u}\|_1, \|\mathrm{div}\mathbf{u}\|_1$, and $\|p\|_1$. Hence

$$\|\tilde{\mathbf{e}}_h\|_{H(\mathrm{div})} \le Ch.$$

An application of the triangle inequality completes the proof for the velocity. The error in the pressure is estimated by invoking the inf-sup condition. ◻

4. Numerical experiments. First note that the error estimate in the main theorem is still valid in the case of the Dirichlet problem. Let us now present some numerical results that illustrate the error behavior of the studied mixed covolume method. The problem was

$$\nabla \cdot (-\mathcal{K}\nabla p) = f(x, y), \quad (x, y) \in \Omega = (0, 1)^2. \tag{4.1}$$

The exact solution was chosen $p = x(1-x)y(1-y)$ and Dirichlet boundary conditions were imposed. The coefficients of the operator were $\mathcal{K} = \mathrm{diag}(k_1, k_2)$, $k_1 = 1+10x^2+y^2$, $k_2 = 1 + x^2 + 10y^2$.

For the flux variable $\mathbf{u} = (u_1, u_2)$ we used the lowest-order Raviart–Thomas piecewise polynomial space $\mathbf{H}_h$ on isosceles right-angled triangles of size h, for $h = 2^{-4}, 2^{-5}, 2^{-6}, 2^{-7}$. The pressure variable p corresponded to piecewise constants on the same triangular elements. The space of piecewise constant is denoted by L_h.

The stiffness matrix and right-hand sides were computed using the following quadrature formula:

$$\int_K \psi \approx \frac{|K|}{3} \left(\psi(m_1) + \psi(m_2) + \psi(m_3)\right). \tag{4.2}$$

Here K is either a primal or a dual triangle (cf. Fig. 2); $|K|$, its area; and m_1, m_2 and m_3, the midpoints of its edges. After the discretization one ends up with the following linear system of equations to be solved:

$$\mathcal{A} \begin{bmatrix} \mathbf{U}_1 \\ \mathbf{U}_2 \\ \mathbf{P} \end{bmatrix} = \underline{\mathbf{f}} = \begin{bmatrix} \boldsymbol{rhs}_{\mathbf{U}_1} \\ \boldsymbol{rhs}_{\mathbf{U}_2} \\ \boldsymbol{rhs}_P \end{bmatrix}, \tag{4.3}$$

with the saddle-point-like stiffness matrix

$$\mathcal{A} = \begin{bmatrix} A & B^T \\ B & 0 \end{bmatrix}. \tag{4.4}$$

We used the fact that $\mathcal{A}$ satisfies the inf-sup condition,

$$\sup_{\mathbf{v},p} \frac{(\mathcal{A}\mathbf{u}, p;\ \mathbf{v}, q)}{\left[\|\mathbf{v}\|^2_{H(\mathrm{div})} + \|q\|_0^2\right]^{\frac{1}{2}}} \ge \beta \left[\|\mathbf{u}\|^2_{H(\mathrm{div})} + \|p\|_0^2\right]^{\frac{1}{2}}, \qquad \forall \mathbf{u},\ p \in \mathbf{H}_h \times L_h, \tag{4.5}$$

TABLE 1
Error behavior and iteration counts for the covolume scheme.

	$h = 1/16$	$h = 1/32$	$h = 1/64$	$h = 1/128$	$\approx$ order
δ_p	2.45e-4	6.17e-5	1.54e-5	3.86e-6	2
δ_{u_1}	5.21e-3	1.25e-3	3.07e-4	7.61e-5	2
δ_{u_2}	5.21e-3	1.25e-3	3.07e-4	7.61e-5	2
$\delta_{u_{\text{int}}}$	3.03e-3	7.70e-4	1.93e-4	4.84e-5	2
# unknowns	1312	5184	20 608	82 176	
# iterations	22	22	23	22	
ϱ	0.37	0.37	0.39	0.38	
κ	2.00	2.09	2.20	2.25	

which in matrix form reduces to the spectral equivalence relations:

$$\left(\mathcal{A}^T \mathcal{A}_0^{-1} \mathcal{A}\underline{\mathbf{x}}, \underline{\mathbf{x}}\right) \geq \beta(\mathcal{A}_0\underline{\mathbf{x}}, \underline{\mathbf{x}}), \qquad \forall \underline{\mathbf{x}} = (\mathbf{U}_1, \mathbf{U}_2, \mathbf{P}). \tag{4.6}$$

Here, $\mathcal{A}_0 = \left[\begin{smallmatrix} A_0 & 0 \\ 0 & I \end{smallmatrix}\right]$ where A_0 corresponds to the stiffness matrix arising from the $H(\text{div})$-bilinear form $\int \mathcal{K}^{-1}\mathbf{u}\cdot\mathbf{v} + \int \text{div}\mathbf{u}\ \text{div}\mathbf{v}$, restricted to the Raviart–Thomas space for the velocity variable.

Then from a general reason it is clear that any preconditioner M of optimal order for A_0 will define an optimal order preconditioner $\mathcal{M} = \left[\begin{smallmatrix} M & 0 \\ 0 & I \end{smallmatrix}\right]$ for $\mathcal{A}$. Recall that $\mathcal{A}$ is nonsymmetric and indefinite. So one can either use $\mathcal{M}$ as a preconditioner in the GMRES or GCG-LS method for $\mathcal{A}$ or one can use $\mathcal{M}$ as a preconditioner to $\mathcal{A}^T\mathcal{M}^{-1}\mathcal{A}$ in the standard CG method. We have chosen in our experiments the first approach. We used a generalized conjugate gradient least squares method (GCG-LS) as derived in [2] (for a mathematically-equivalent-to-the-GMRES method, see Saad [21]).

Choices of M, a preconditioner for the $H(\text{div})$-bilinear form are found in [3, 22, 1]. We used in the experiments reported in Table 1 an algebraically stabilized version of the hierarchical method from [3]. Details on the algebraic stabilization of the HB methods are found, for example, in [23].

The stopping criterion in the GCG-LS method was

$$\|\mathcal{M}^{-\frac{1}{2}}\mathcal{A}\mathbf{r}\| \leq 10^{-9}\|\mathcal{M}^{-\frac{1}{2}}\mathcal{A}\mathbf{r}_0\|,$$

where $\|\mathbf{v}\|^2 = \mathbf{v}^T\mathbf{v}$, and $\mathbf{r}_0$ stands for the initial residual, $\mathbf{r}$ is the current one. The initial iterate was chosen as $\mathbf{x}_0 = \mathcal{M}^{-1}\mathbf{f}$, where $\mathbf{f}$ was the right-hand side of the discrete problem $\mathcal{A}\mathbf{x} = \mathbf{f}$.

We show in Table 1, in addition to the error behavior of the covolume discretization method, also ϱ, κ and the number of iterations, where

$$\varrho = \left(\frac{\|\mathcal{M}^{-\frac{1}{2}}\mathcal{A}\boldsymbol{r}\|}{\|\mathcal{M}^{-\frac{1}{2}}\mathcal{A}\boldsymbol{r}_0\|}\right)^{1/\#\text{ iterations}} \tag{4.7}$$

was an average reduction factor, and κ was the condition number of $\mathcal{M}^{-1}\mathcal{A}_0$. Recall that $\mathcal{A}_0 = \left[\begin{smallmatrix} A_0 & 0 \\ 0 & I \end{smallmatrix}\right]$, where A_0 stands for the matrix corresponding to the $H(\text{div})$-bilinear form $(\mathcal{K}^{-1}\mathbf{u}, \mathbf{v})+(\text{div}\mathbf{u},\ \text{div}\mathbf{v})$ computed from the triangular Raviart–Thomas velocity space.

More specifically, denote $x_i = ih_x$, $y_j = jh_y$, $i = 0, 1, 2, \ldots, n_x$, $j = 0, 1, 2, \ldots, n_y$, $h_x = h_y = h$, $n_x = n_y = n = 1/h$, for a given $h = 2^{-4}, 2^{-5}, 2^{-6}, 2^{-7}$. In Table 1, we show

Table 2
Error behavior and iteration counts for the standard mixed finite element scheme.

	$h = 1/16$	$h = 1/32$	$h = 1/64$	$h = 1/128$	$\approx$ order
δ_p	2.84e-4	7.14e-5	1.79e-5	4.47e-6	2
δ_{u_1}	5.21e-3	1.25e-3	3.07e-4	7.61e-5	2
δ_{u_2}	5.21e-3	1.25e-3	3.07e-4	7.61e-5	2
$\delta_{u_{\text{int}}}$	3.03e-4	7.70e-4	1.93e-4	4.84e-5	2
# unknowns	1312	5184	20 608	82 176	
# iterations	22	22	23	22	
ϱ	0.37	0.38	0.39	0.38	
κ	2.00	2.09	2.20	2.25	

(i)

$$\begin{aligned}\delta_p &= \|I_h p - p_h\|_h \\ &:= \left[\sum_{i=1}^{n_x}\sum_{j=1}^{n_y} h_x h_y \Big(p\Big(x_i - \frac{1}{2}h_x, y_j - \frac{1}{2}h_y\Big) - p_h\Big(x_i - \frac{1}{2}h_x, y_j - \frac{1}{2}h_y\Big)\Big)^2\right]^{\frac{1}{2}},\end{aligned}$$

i.e., a discrete L^2-norm of the error $p - p_h$;

(ii)

$$\begin{aligned}\delta_{u_1} &= \|I_h u_1 - u_{h,\,1}\|_h \\ &:= \left[\sum_{i=0}^{n_x}\sum_{j=1}^{n_y} h_x h_y \Big(u_1\Big(x_i, y_j - \frac{1}{2}h_y\Big) - u_{h,\,1}\Big(x_i, y_j - \frac{1}{2}h_y\Big)\Big)^2\right]^{\frac{1}{2}},\end{aligned}$$

i.e., a discrete L^2-norm of the error $u_1 - u_{h,1}$;

(iii)

$$\begin{aligned}\delta_{u_2} &= \|I_h u_2 - u_{h,\,2}\|_h \\ &:= \left[\sum_{i=1}^{n_x}\sum_{j=0}^{n_y} h_x h_y \Big(u_2\Big(x_i - \frac{1}{2}h_x, y_j\Big) - u_{h,\,2}\Big(x_i - \frac{1}{2}h_x, y_j\Big)\Big)^2\right]^{\frac{1}{2}},\end{aligned}$$

i.e., a discrete L^2-norm of the error $u_2 - u_{h,\,2}$;

(iv)

$$\delta_{u_{\text{int}}} = \|I_h(\mathbf{u} - \mathbf{u}_h)\|_h$$

$$:= \left[\sum_{i=1}^{n_x}\sum_{j=0}^{n_y} h_x h_y \Big((\mathbf{u}\cdot\mathbf{n})\Big(x_i - \frac{1}{2}h_x, y_j - \frac{1}{2}h_y\Big) - (\mathbf{u}_h\cdot\mathbf{n})\Big(x_i - \frac{1}{2}h_x, y_j - \frac{1}{2}h_y\Big)\Big)^2\right]^{\frac{1}{2}},$$

i.e., a discrete L^2-norm of the error $\mathbf{u}\cdot\mathbf{n} - \mathbf{u}_h\cdot\mathbf{n}$, where $\mathbf{n}$ is the unit normal vector to the edge $(x_{i-1}, y_{j-1}),\ (x_i, y_j)$;

(v) the number of iterations of the preconditioned GCG-LS method;

(vi) the average reduction factors ϱ, (4.7);

(vii) the condition number κ of $\mathcal{M}^{-1}\mathcal{A}_0$;

(viii) the total number of unknowns (for both $\mathbf{U}$ and $\mathbf{P}$).

It turns out that our experiments suggest second-order approximation in all variables. Notice also the constant number of iterations (and corresponding average reduction factors ϱ) in the preconditioned GCG-LS method.

For comparison, in Table 2, we have included the same kind of results as reported in Table 1, now for the standard mixed finite element scheme. One can observe that the schemes differ very little; the covolume one admits slightly better error behavior for the pressure variable p.

REFERENCES

[1] D. N. Arnold, R. S. Falk, and R. Winther, *Preconditioning in H(div) and applications*, Math. Comp., 66 (1997), pp. 957–984.

[2] O. Axelsson, *Iterative Solution Methods*, Cambridge University Press, Cambridge, 1994.

[3] Z. Cai, C. I. Goldstein, and J. E. Pasciak, *Multilevel iteration for mixed finite element systems with penalty*, SIAM J. Sci. Comput., 14 (1993), pp. 1072–1088.

[4] Z. Cai, J. E. Jones, S. F. McCormick, and T. F. Russell, *Control-volume mixed finite element methods*, Comput. Geosci., to appear.

[5] S. H. Chou, *Analysis and convergence of a covolume method for the generalized Stokes problem*, Math. Comp., 66 (1997), pp. 85–104.

[6] S. H. Chou and D. Y. Kwak, *Analysis and convergence of a MAC-like scheme for the generalized Stokes problem*, Numer. Methods Partial Differential Equations., 13 (1997), pp. 1–16.

[7] S. H. Chou and D. Y. Kwak, *Mixed covolume methods on rectangular grids for elliptic problems*, SIAM J. Numer. Anal., submitted.

[8] S. H. Chou and Q. Li, *Error estimates in L^2, H^1 and L^∞ in covolume methods for elliptic and parabolic problems: A unified approach*, Math. Comp., submitted.

[9] S. H. Chou and D. Y. Kwak, *A covolume method based on rotated bilinears for the generalized Stokes problem*, SIAM J. Numer. Anal., 35 (1998), pp. 494–507.

[10] S. H. Chou, D. Y. Kwak, and P. Vassilevski, *Mixed covolume methods on rectangular grids for convection dominated problems*, SIAM J. Sci. Comput., submitted.

[11] S. H. Chou and P. S. Vassilevski, *An upwinding cell–centered method with piecewise constant velocity over covolumes*, Numer. Methods Partial Differential Equations, to appear.

[12] S. H. Chou and P. S. Vassilevski, *A general mixed co–volume framework for constructing conservative schemes for elliptic problems*, Math. Comp., to appear.

[13] C. A. Hall, T. A. Porsching, and P. Hu, *Covolume-dual variable method for thermally expandable flow on unstructured triangular grids*, Comp. Fluid Dynamics, 2 (1994), pp. 111–139.

[14] F. H. Harlow and F. E. Welch, *Numerical calculations of time dependent viscous incompressible flow of fluid with a free surface*, Phys. Fluids, 8 (1965), p. 2181.

[15] R. A. Nicolaides, *Direct discretization of planar div-curl problems*, SIAM J. Numer. Anal., 29 (1992), pp. 32–56.

[16] R. A. Nicolaides, *Analysis and convergence of the MAC scheme*, SIAM. J. Numer. Anal., 29 (1992), pp. 1579–1591.

[17] R. A. Nicolaides, T. A. Porsching, and C. A. Hall, *Covolume methods in computational fluid dynamics,* in Computational Fluid Dynamics Review, M. Hafez and K. Oshma, eds., John Wiley, New York, 1995, pp. 279–299.

[18] J. Roberts and J. Thomas, *Mixed and hybrid methods*, in Handbook of Numerical Analysis Vol II, Chapter 4, P. G. Ciarlet and J. L. Lions, eds., North–Holland, Amsterdam, 1991.

[19] T. F. Russel and M. Wheeler, *Finite element and finite difference methods for continuous flows in porous media*, in The Mathematics of Reservoir Simulation, Frontiers in Applied Mathematics 1, R. E. Ewing, ed., SIAM, Philadelphia, 1984.

[20] T. F. Russell, *Rigorous Block-Centered Discretizations on Irregular Grids: Improved Simulation of Complex Reservoir Systems*, Tech. report No. 3, Project Report, Reservoir Simulation Research Corporation, Denver, CO, 1995.

[21] Y. Saad, *Iterative Methods for Sparse Linear Systems*, PSW Publishing Co., Boston, MA, 1995.

[22] P. S. Vassilevski and J. Wang, *Multilevel iterative methods for mixed finite element discretizations of elliptic problems*, Numer. Math., 63 (1992), pp. 503–520.

[23] P. S. Vassilevski, *On two ways of stabilizing the hierarchical basis methods*, SIAM Rev., 39 (1997), pp. 18–53.